Solid flexible electrochemical supercapacitor using Tobacco mosaic virus nanostructures and ALD…

6 authors, including:

Markus Gnerlich
University of Maryland, College Park
15 PUBLICATIONS   **95** CITATIONS

Ekaterina A. Pomerantseva
Drexel University
55 PUBLICATIONS   **989** CITATIONS

Keith Gregorczyk
University of Maryland, College Park
27 PUBLICATIONS   **437** CITATIONS

Gary Rubloff
University of Maryland, College Park
311 PUBLICATIONS   **8,977** CITATIONS

Solid flexible electrochemical supercapacitor using *Tobacco mosaic* virus nanostructures and

ALD ruthenium oxide

Solid flexible electrochemical supercapacitor using *Tobacco mosaic* virus nanostructures and ALD ruthenium oxide

M Gnerlich[1,2,5]**, E Pomerantseva**[1,2]**, K Gregorczyk**[2,3]**, D Ketchum**[4]**,
G Rubloff**[2,3] **and R Ghodssi**[1,2,3,5]

[1] Department of Electrical and Computer Engineering, University of Maryland, College Park,
MD 20742, USA
[2] Institute for Systems Research, University of Maryland, College Park, MD 20742, USA
[3] Department of Materials Science and Engineering, University of Maryland, College Park, MD 20742,
USA
[4] Laboratory for Physical Sciences, College Park, MD 20740, USA

E-mail: ghodssi@umd.edu and gnerlich@umd.edu

Abstract
An all-solid electrochemical supercapacitor has been developed using a nanostructured nickel
and titanium nitride template that is coated with ruthenium oxide by atomic layer deposition
(ALD). The electrode morphology was based on a high surface area biotemplate of genetically
modified *Tobacco mosaic* virus. The biotemplate automatically self-assembles at room
temperature in aqueous solution. Nafion® perfluorosulfonate ionomer dispersion was cast on
the electrodes and used as a solid proton-conducting electrolyte. A 5.8 F g^{-1} gravimetric
capacity (578 μF cm^{-2} based on footprint) was achieved in Nafion electrolyte, and the device
retained 80% of its capacity after 25 000 cycles. The technology presented here will enable
thin, solid, flexible supercapacitors that are compatible with standard microfabrication
techniques.

(Some figures may appear in colour only in the online journal)

1. Introduction

Supercapacitors store electrical energy in an electronic double layer (EDL) and/or through a surface redox reaction, referred to as EDLC or pseudocapacitors, respectively. The charge storage mechanisms are very rapid and highly reversible compared to rechargeable batteries, leading to their use in high power density applications [1, 2]. Current research trends are focused on improving energy density of supercapacitors, either by increasing surface area of EDLC using new nanomaterials or investigating electrolytes with higher voltage windows. Carbons are most frequently used for EDLC electrodes due to their high surface area, low cost and manufacturability [3], but further increasing surface area can come at the expense of ionic mobility in the constrained nanogeometries. A library

of transition metal oxides are available as redox materials for pseudocapacitors, of which ruthenium oxide (RuO$_2$) is attractive due to its high gravimetric capacity (720 F g^{-1} [4] to 977 F g^{-1} [5]), intrinsic electronic conductivity (37 $\mu\Omega \cdot$ cm [6]), and chemical stability in acidic electrolytes. For more information on RuO$_2$ the following reviews are recommended: [5, 7, 8].

Typically, energy storage in pseudocapacitors involves surface mechanisms, but the capacity can be increased by using redox materials that allow the bulk of the material to participate. The chemical reaction for energy storage in hydrated RuO$_2$ involves protons and electrons, and optimally prepared RuO$_2 \cdot$ xH$_2$O is able to conduct both. This approach minimizes unused volume and maximizes energy density. An alternative approach to make efficient use of RuO$_2$ is deposition on a nanostructured high surface area template causing a large portion of the RuO$_2$ surface to be in direct

---

[5] Authors to whom any correspondence should be addressed.

contact with electrolyte. Such an electrode has been created from genetically modified *Tobacco mosaic* virus (TMV) which self-assembles onto a prepared substrate at room temperature and is easily metalized for further processing [9, 10]. Onto this high surface area biotemplate, RuO_2 thin film was deposited by atomic layer deposition (ALD), a technique well known for its conformality and monolayer thickness control [11]. The drawback of this approach is that ALD methods to deposit hydrated RuO_2 are not available, and the RuO_2 film is anhydrous resulting in reduced gravimetric capacity [12]. Nevertheless, the combination of ALD energy storage materials with TMV has been demonstrated to be a powerful method for producing nanostructured lithium-ion battery electrodes [13, 14] and is expected to be important for new supercapacitor technologies as well.

In this work RuO_2 nanostructures were synthesized through biotemplating and used in a supercapacitor fabricated from solid, flexible materials. DuPont Nafion®—a solid sulfonated polymer—was used as a proton-conducting electrolyte. The combination of a polyimide substrate, TMV-enhanced current collector, RuO_2 and Nafion electrolyte provides a platform to optimize our vision of a thin, solid, flexible supercapacitor.

2. Methods

2.1. Supercapacitor design

The objective of this design is integration of a supercapacitor with a top–down microfabrication process for complex microfabricated systems. The starting substrate is a Si wafer with a flexible, insulating polyimide coating. A metal current collector (Ti/Au) is deposited on the polyimide, and surface area is increased using TMV-1Cys. TMV-1Cys is a genetically modified version of TMV containing a cysteine residue in the coat protein that causes the virus to adhere to surfaces with a preferential vertical orientation. The cysteine residue also provides numerous metal binding sites that allow for the formation of a continuous Ni shell by electroless Ni plating. This procedure rigidly fixes the biotemplate in place and converts the non-conductive TMV-1Cys into a conductive high surface area electrode [9]. A conductive titanium nitride (TiN) layer is then deposited by ALD to protect the Ni from the acidic electrolyte. RuO_2 is also deposited by ALD on the TMV-1Cys/Ni/TiN current collector. A schematic of the design is shown in figure 1. Previous research has demonstrated supercapacitors based on RuO_2 powders with Nafion used either as a solid electrolyte [15] [17] or a binder [16] with liquid electrolyte. In contrast, the RuO_2 thin film in this work is directly deposited on electrodes that have very high surface area. Each electrode is identical and symmetrical in geometry. The silicon substrate may be removed by a silicon etch to release the flexible device.

2.2. Fabrication process

Fabrication of the biotemplated RuO_2 electrode begins with a silicon wafer used as a substrate and coated with a flexible spin-on polyimide precursor (HD Microsystems HD-4110) that is
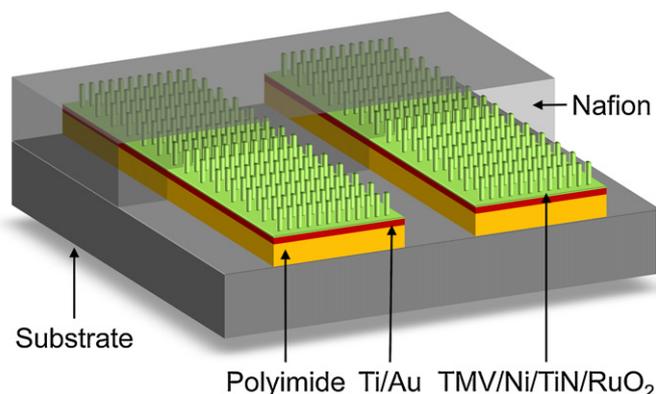
Figure 1. Cross-section schematic of the supercapacitor showing silicon substrate, polyimide insulator, Ti/Au current collector and RuO_2 coating on TMV-1Cys/Ni/TiN template. The symmetrical electrodes are arranged in an interdigitated pattern and the entire structure is encapsulated in solid Nafion electrolyte.

vacuum baked at 375 °C to produce a polyimide insulator. A schematic diagram of the fabrication process is shown in figure 2. Next, the polyimide is roughed in oxygen plasma (Plasma-Therm 790) and coated with a Ti/Au (200 Å/2000 Å) layer in an e-beam evaporator (CHA Industries). Each wafer was diced into 1 cm by 1 cm chips before coating with TMV-1Cys. The TMV-1Cys was prepared as reported previously [9].

Each chip was submerged in a 0.2 g L^{-1} suspension of the TMV-1Cys in 0.1 M phosphate buffer, and the biotemplate was allowed to assemble overnight. The excess TMV-1Cys solution was removed and a 12:1 solution of phosphate buffer and sodium tetrachloropalladate ($NaPdCl_4$) was added to functionalize the TMV-1Cys surface for electroless metallization. The palladium solution was removed, and an aqueous nickel plating solution of $NiCl_2$, glycine, $Na_2B_4O_7$ and dimethylamine borane (DMAB) was added. The nickel plating reaction is autocatalyzed but starts at the palladium functionalized TMV-1Cys to produce a coating of nickel. The reaction stops when the sample is removed from solution and rinsed with water.

TiN was deposited on the TMV-1Cys/Ni template by 200 cycles of TDMAT and ammonia at 175 °C in a Beneq TFS 500 ALD system. RuO_2 was deposited on the TMV biotemplate by ALD using 2000 cycles of bis(2,2,6 trimethyl cyclohexadienyl)-ruthenium and oxygen in a custom built, cross flow reactor at 225 °C [18]. Samples were weighed with a microgram-precision analytical balance (Mettler Toledo, XS105) before and after coating to determine total mass loading, which was between 199 and 266 $\mu g\ cm^{-2}$ for various chips.

Supercapacitors were prepared by creating an interdigitated pattern by mechanically scribing through the material stack using a probe station, exposing the underlying silicon substrate while separating the electrically isolated electrodes. The devices were 8 mm by 8 mm and each electrode is approximately 1 mm wide and 6 mm long. The separation between electrodes was approximately 60 μm, measured during SEM inspection prior to Nafion coating. Nafion dispersion (Ion Power) was spin coated on the chip, solidified at 70 °C on a hotplate and annealed for 4 h at 140 °C in a nitrogen purged

	Silicon substrate is spin coated with polyimide precursor, baked and metallized with Ti/Au
	TMV-1Cys self-assembles on metal surface and is coated with nickel by electroless deposition
	TMV-1Cys/Ni is coated with TiN (200 cycles ALD) and then with RuO$_2$ (2000 cycles ALD)
	Electrodes are electrically isolated
	Nafion dispersion is spin-coated and annealed
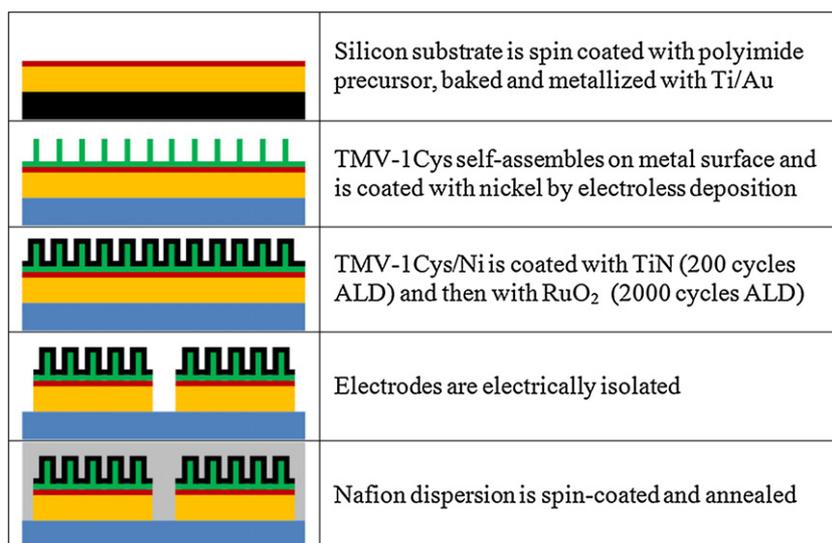
Figure 2. Fabrication process flow of the biotemplated supercapacitor electrodes.

ramping furnace (Lindberg/Blue M BF51732BC). Nafion was removed from the electrical contact pads by swabbing with isopropyl alcohol. The Nafion thickness was measured to be approximately 20 μm by a step profilometer (Veeco Dektak 6M) on a sacrificial device that was scribed through the Nafion.

2.3. Testing apparatus

Protonation of the RuO$_2$ surface enables energy storage through an oxidation state change that involves transfer of electrons—a process that can be reversed with an applied voltage. The energy storage capability of the supercapacitor is demonstrated using Nafion. The ionic behavior of Nafion is complex [19], but it generally requires some absorbed water content to maximize ionic conductivity. Electrochemical tests were performed with the supercapacitor in a symmetrical configuration without a reference electrode. To evaluate supercapacitor performance three types of tests using cyclic voltammetry were conducted (BioLogic VSP potentiostat). First, repeated cyclic voltammetry tests were completed with the devices in a controlled temperature/humidity chamber (Espec SH-241). A custom holder was used based on a 50 mL centrifuge tube with spring clips that provided electrical contact and mechanical support. The bottom portion of the tube was removed to expose the chip to the environmental chamber (see figure 3). Second, TMV-templated electrodes without an interdigitated pattern and without Nafion were tested by submerging in 0.5 M H$_2$SO$_4$. Third, cycle lifetime tests on interdigitated electrodes with Nafion were completed while the devices were suspended in a sealed 50 mL test tube. The test tube contained either ambient air or a few milliliters of deionized water (DI) to make a humidified test chamber.

3. Results

3.1. Electrode characterization

The structure of the electrode produced by metalized TMV was evaluated by SEM and shows a high surface area
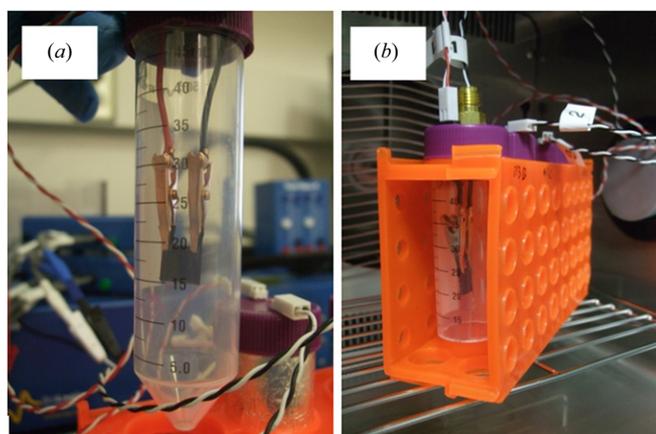
Figure 3. Characterization takes place in a 50 mL test tube with clips connecting the electrodes to the potentiostat. (*a*) For 'ambient' test the tube is sealed in the lab and (*b*) for controlled temp/humidity the bottom of the tube is cut off and placed in an environmental chamber.

electrode ideal for supercapacitors (figure 4). TEM images and EDS spectra (JEOL 2100F) were extracted from nanoparticle samples transferred from the electrode surface to a TEM grid. The cross-section obtained by TEM (figure 5) demonstrates the layered structure of TMV-1Cys/Ni/TiN/RuO$_2$. The EDS spectrum overlay shows the core from the initial TMV-1Cys particle is 20 nm with a 30 nm nickel coating. The TiN layer is 10–20 nm and the RuO$_2$ layer is 20–30 nm. It was found that the TiN coating dramatically increased the RuO$_2$ loading compared to nickel alone, and it also protects the nickel from acidic electrolytes thereby increasing the cycle lifetime. The composition of the RuO$_2$ coating was evaluated by powder XRD (Brucker D8 Advance) showing the presence of polycrystalline RuO$_2$ (figure 6(*a*)).
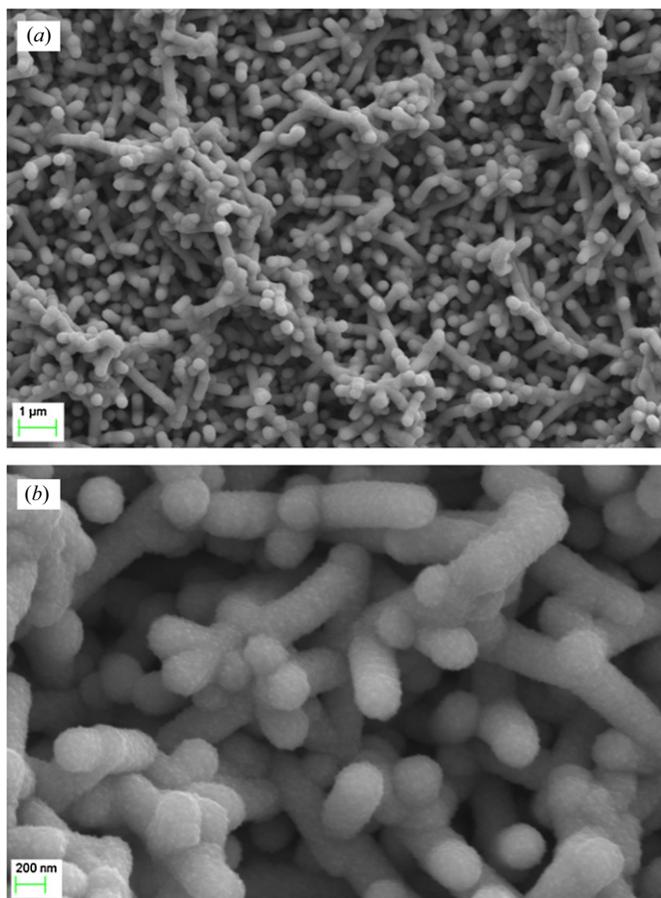
Figure 4. SEM image at (*a*) 50 KX and (*b*) 200 KX of TiN and RuO$_2$ deposited by ALD on TMV-1Cys templated nickel.

Figure 5. (*a*) TEM image of a 160 nm diameter TMV-1Cys/Ni/TiN/RuO$_2$ nanoparticle showing the multilayer structure. (*b*) EDX spectrum linescan overlaid on corresponding TEM image.

3.2. Electrode testing

3.2.1. Solid electrolyte. The devices were tested by cyclic voltammetry from 1 to 500 mV s^{-1} and the capacitance was extracted from current measured at the zero voltage crossing using $C = i/(\mathrm{d}V/\mathrm{d}t)$. Since the ionic conduction of Nafion is a strong function of the water content of the polymer, it is expected that capacity at a particular scan rate would decrease as humidity decreases. The cyclic voltammetry tests in Nafion (figure 7) indicate a maximum capacity of 5.8 F g^{-1} at 2 mV s^{-1} where the mass is based on the mass loading and the area of a single electrode. The areal capacity is 578 μF cm^{-2} based on total footprint area of the device.

Although the gravimetric capacity is low compared to hydrous RuO$_2$ powders, the stability of the RuO$_2$/Nafion supercapacitors is quite good. The devices were tested in either ambient or 100% relative humidity by adding a small amount of DI water to a sealed test tube (the environmental chamber was not used for this test). Cyclic voltammetry at 50 mV s^{-1} was repeated for up to 25 000 cycles (see figure 8), and the total charge per cycle was evaluated using BioLogic EC-Lab v10.3 software. The capacity of the supercapacitor in high humidity was higher at the very beginning of the test, but the capacity after a few thousand cycles was similar to the device exposed to ambient humidity. The cycle lifetime was poorer in a high humidity environment, and the unusual behavior shown in figure 8 after 15 000 cycles is likely due to

interfacial failure and subsequent degradation of the current collector. Possible reasons for this behavior are incomplete coverage of the current collector by TiN, as well as mechanical stress caused by swelling of Nafion at high humidity. At ambient humidity levels the supercapacitor retained 80% of charge/discharge capability after 25 000 cycles.

An estimate of the internal parasitic resistance was made with the potentiostat (input impedance of 10^{12} Ω) from a simple self-discharge test after charging to 0.5 V using 10 μA of current. The time constant indicates this resistance to be 9.4 MΩ between the electrodes.

3.2.2. Liquid electrolyte. In addition to tests in Nafion electrolyte, the supercapacitor electrodes were tested in 0.5 M H$_2$SO$_4$ in a symmetrical configuration without a reference electrode (figure 9). A significantly larger capacity of 47 F g^{-1} at 1 mV s^{-1} resulted from the test in 0.5 M H$_2$SO$_4$ than resulted from Nafion. It must be noted that the cycle lifetime in aqueous H$_2$SO$_4$ was poor and it appeared that delamination occurred between the Au/Ni interface. This is probably due to dissolution of the Ni in areas that are not completely covered by TiN and RuO$_2$.

4. Discussion

The Ni-coated self-assembled TMV-1Cys biotemplate enables the production of a stable, nanostructured, high surface area
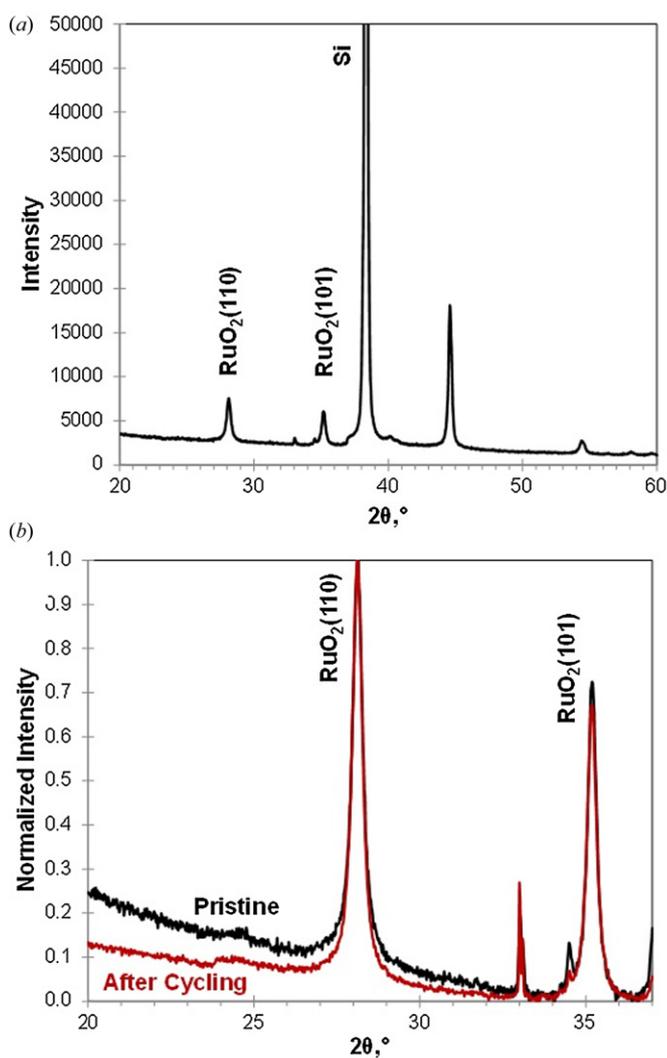
Figure 6. (*a*) XRD pattern of RuO$_2$ deposited by ALD on TMV-1Cys/Ni/Ti on a Si/polyimide/Ti/Au substrate. The RuO$_2$ peaks were identified by [22] and the large Si peak is due to the substrate. (*b*) Comparison of XRD patterns of RuO$_2$ before and after electrochemical testing in 0.5 M H$_2$SO$_4$.

Figure 7. Cyclic voltammetry curves for RuO$_2$ on TMV-1Cys/Ni/TiN current collector with Nafion in (*a*) 30% RH and (*b*) 80% RH at scan rates of 1, 10, 100, and 500 mV s^{-1}. The TMV-templated interdigitated electrodes are in a symmetrical configuration.

current collector suitable for microfabricated supercapacitor electrodes, and RuO$_2$ active material was deposited by ALD. This fabrication approach allows the energy density behavior of this complex system to be studied by electrochemical characterization in liquid and solid electrolytes. A comparison of the specific capacitance as a function of scan rate for these electrolytes is shown in figure 10.

Overall, the measured gravimetric capacities are lower than reported values for hydrated RuO$_2$, which ranges from 527 to 900 F g^{-1} [12] depending on the annealing temperature. The capacity of RuO$_2$ is highly dependent on the hydration state, the deposition method, the substrate's surface area and particle size. The capacity of solid anhydrous RuO$_2$ is less than 1 F g^{-1} and increases to between 19 and 29 F g^{-1} with small amounts of water in the structure [12]. Although RuO$_2$ prepared by the ALD method does not contain water, it is a thin film deposited on the nanostructured TMV biotemplate and has significant surface area. Mesoporous anhydrous RuO$_2$ tested by cyclic voltammetry in H$_2$SO$_4$ was found to

have a specific capacity between 29–58 F g^{-1} depending on scan rate [20], and the specific capacity of RuO$_2$ powders depends strongly on the particle size [21]. Furthermore, the measured capacity of the anhydrous RuO$_2$ film may be higher than 1 F g^{-1} due to the grain structure visible in the other RuO$_2$ layer in figure 5. Such morphology may allow ions to penetrate the surface of the RuO$_2$ and more material would be electrochemically active compared to a homogeneous film. Pristine chips and chips from the same fabrication run after cyclic voltammetry in 0.5 M H$_2$SO$_4$ were compared by XRD (figure 6(*b*)), showing little change in the structure. A shift in the peak position would be expected if water and/or protons were able to penetrate the surface of RuO$_2$ during cyclic voltammetry at slow scan rates. Therefore the capacity of the RuO$_2$ in H$_2$SO$_4$ is likely due to the nanostructure of the TMV biotemplate, and the comparatively lower capacity in Nafion is likely due ionic conductivity rate limitations of the polymer electrolyte.

In order to determine whether the measurement from cyclic voltammetry was primarily Faradaic (redox) or non-Faradaic (capacitive), the cyclic voltammetry sweep rate was
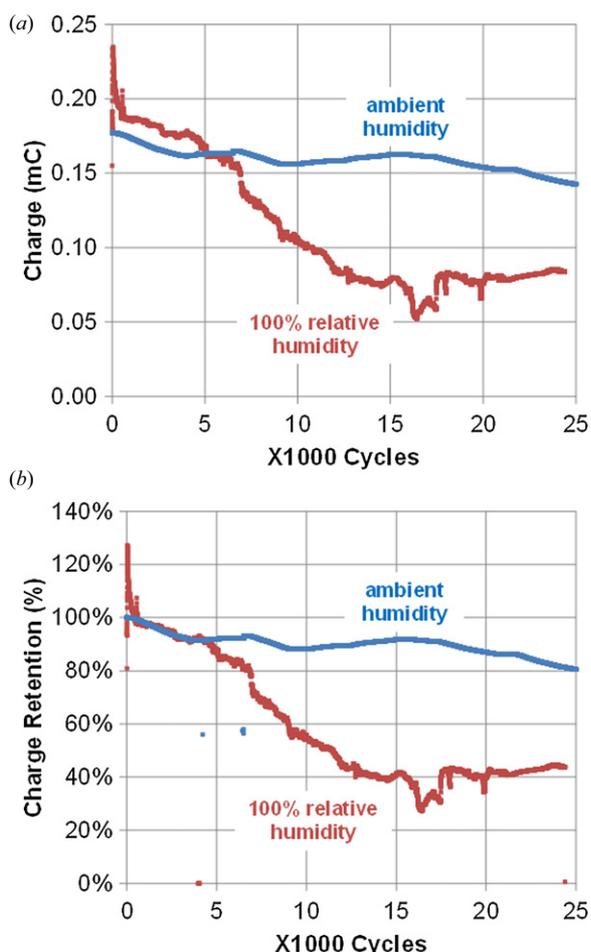
Figure 8. Plot of (*a*) total charge capability (measured by cyclic voltammetry at 50 mV s^{-1}) and (*b*) charge retention over 25 000 cycles for RuO$_2$/Nafion supercapacitor with TMV-1Cys/Ni/TiN current collector in ambient humidity and 100% relative humidity.
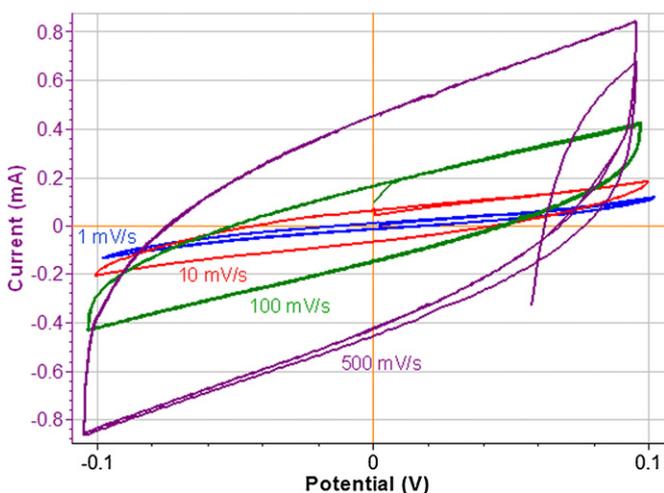
Figure 9. Cyclic voltammetry curves for RuO$_2$ on TMV-1Cys/Ni/TiN current collector with 0.5 M H$_2$SO$_4$ at scan rates of 1, 10, 100, 500 mV s^{-1}. The TMV-templated electrodes are in a symmetrical configuration without a reference electrode.

varied from 1–500 mV s^{-1}. The current due to a Faradaic reaction can be calculated from the Randles–Sevcik equation
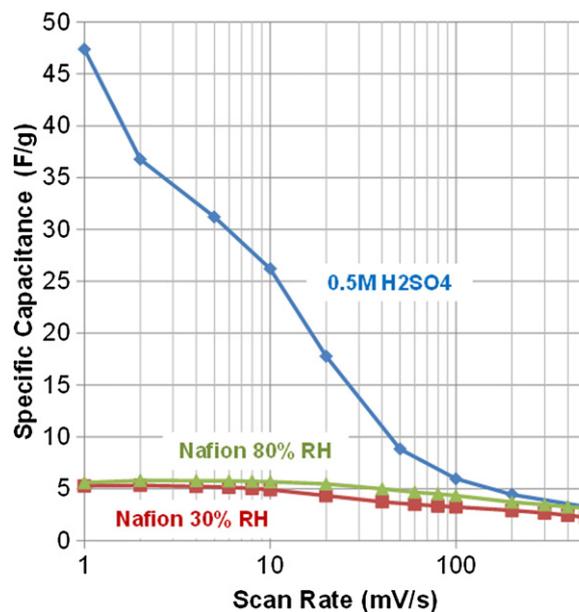
Figure 10. A comparison of the derived specific capacitances from cyclic voltammetry curves in liquid and solid electrolyte at rates of 1 to 500 mV s^{-1}.

for redox current, which in simplified form at 25 °C is given by equation (1) where n is the number of electrons appearing in redox half-reaction, dv/dt is the scan rate, D is the ionic diffusion coefficient, A is the electrode area, C is the ionic concentration:

$$i = 2.687 \times 10^5 n^{1.5} \left(\frac{\mathrm{d}v}{\mathrm{d}t} \right)^{0.5} D^{0.5} AC. \tag{1}$$

The current due to the EDLC is purely capacitive in nature and is given by equation (2), where C is the capacitance (F):

$$i = C \frac{\mathrm{d}v}{\mathrm{d}t}. \tag{2}$$

If the current is proportional to scan rate to the 0.5 power, the charge storage mechanism is Faradaic, and if it is proportional the 1.0 power, the charge storage mechanism is non-Faradaic. An intermediate value indicates a combination of both mechanisms. A power law fit to the results in 0.5 M H$_2$SO$_4$ as a function of scan rate was $x^{0.54}$ indicating primarily Faradaic capacity. On the other hand, a power law fit to the capacity in Nafion as a function of scan rate was $x^{0.84}$ indicating a mix of Faradaic and non-Faradaic mechanisms. The overall smaller capacity of the supercapacitor in Nafion may be related to lower ionic transport which would limit the redox reaction with RuO$_2$. Ionic transport limitations due to poor electrolyte contact with RuO$_2$ are unlikely since the Nafion is applied as a liquid dispersion, and it is quite difficult to remove.

Since the present design uses closely spaced interdigitated electrodes and no separator, the leakage current may be decreased only by increasing electrode spacing. However this also increased the distance ions must move through the electrolyte. Future work will focus on optimizing the interdigitated electrode geometry and Nafion coating in order to decrease leakage current and improving proton transport.

5. Conclusion

A nanostructured supercapacitor electrode was fabricated from TMV-1Cys, Ni and TiN and combined with ALD to provide a new pathway to deposit active supercapacitor materials such as RuO_2 on a high surface area current collector. Using this technique, biotemplated RuO_2 with 5.8 F g^{-1} gravimetric capacity (578 μF cm^{-2} based on footprint) was achieved in Nafion electrolyte. The device retained 80% of its capacity after 25 000 cycles. Future work will include the optimization of electrode geometry, investigation of alternate methods of RuO_2 deposition on TMV-1Cys that allow incorporation of H_2O, and demonstration of a fully flexible supercapacitor after release from the microfabrication substrate.

Acknowledgments

References

[1] Morimoto T, Hiratsuka K, Sanada Y and Kurihara K 1995 Electric double-layer capacitor using organic electrolyte *J. Power Sources* **60** 239–47

[2] Lokhande C D, Dubal D P and Joo O 2011 Metal oxide thin film based supercapacitors *Curr. Appl. Phys.* **11** 255–70

[3] Frackowiak E 2007 Carbon materials for supercapacitor application *Phys. Chem. Chem. Phys.* **9** 1774–85

[4] Zheng J P and Jow T R 1995 A new charge storage mechanism for electrochemical capacitors *J. Electrochem. Soc.* **142** L6–8

[5] Liu X and Pickup P G 2008 Ru oxide supercapacitors with high loadings and high power and energy densities *J. Power Sources* **176** 410–6

[6] Jia Q X, Song S G, Wu X D, Cho J H, Foltyn S R, Findikoglu A T and Smith J L 1996 Epitaxial growth of highly conductive RuO_2 thin films on (1 0 0) Si *Appl. Phys. Lett.* **68** 1069–71

[7] Kötz R and Carlen M 2000 Principles and applications of electrochemical capacitors *Electrochim. Acta* **45** 2483–98

[8] Sherrill S A, Banerjee P, Rubloff G W and Lee S B 2011 High to ultra-high power electrical energy storage *Phys. Chem. Chem. Phys.* **13** 20714–23

[9] Royston E, Ghosh A, Kofinas P, Harris M T and Culver J N 2008 Self-assembly of virus-structured high surface area nanomaterials and their application as battery electrodes *Langmuir* **24** 906–12

[10] Gerasopoulos K, McCarthy M, Banerjee P, Fan X, Culver J N and Ghodssi R 2012 Biofabrication methods for the patterned assembly and synthesis of viral nanotemplates *Nanotechnology* **21** 055304

[11] George S M, Ott A W and Klaus J W 1996 Surface chemistry for atomic layer growth *J. Phys. Chem.* **100** 13121–31

[12] McKeown D A, Hagans P L, Carette L P P, Russel A E, Swider K E and Rolison D R 1999 Structure of hydrous ruthenium oxides: implications for charge storage *J. Phys. Chem.* B **103** 4825–32

[13] Gerasopoulos K, Chen X, Culver J N, Wang C and Ghodssi R 2010 Self-assembled Ni/TiO_2 nanocomposite anodes synthesized via electroless plating and atomic layer deposition on biological scaffolds *Chem. Commun.* **46** 7349–51

[14] Pomerantseva E, Gerasopoulos K, Chen X, Rubloff G and Ghodssi R 2012 Electrochemical performance of the nanostructured biotemplated V_2O_5 cathode for lithium-ion batteries *J. Power Sources* **206** 282–7

[15] LaConti A B, Sarangapani S, Kosek J A and Forchione J 1992 Proton exchange membrane electrochemical capacitors and fuel cells for pulse power applications *IEEE 35th Int. Power Sources Symp.* pp 298–301

[16] Qin X, Durbach S and Wu G T 2004 Electrochemical characterization on $RuO_2 \cdot xH_2O$/carbon nanotubes composite electrodes for high energy density supercapacitors *Carbon* **42** 423–60

[17] Park K-W, Ahn H-J and Sung Y-E 2002 All-solid-state supercapacitor using a Nafion polymer membrane and its hybridization with a direct methanol fuel cell *J. Power Sources* **109** 500–6

[18] Gregorczyk K, Henn-Lecordier L, Gatineau J, Dussarrat C and Rubloff G 2011 Atomic layer deposition of ruthenium using the novel precursor bis(2,6,6-trimethyl-cyclohexadienyl)ruthenium *Chem. Mater.* **23** 2650–6

[19] Mauritz K A and Moore R B 2004 State of understanding of Nafion *Chem. Rev.* **104** 4535–85

[20] Subramanian V, Hall S C, Smith P H and Rambabu B 2004 Mesoporous anhydrous RuO_2 as a supercapacitor electrode material *Solid State Ion.* **175** 511–5

[21] Sugimoto W, Yokoshima K, Murakami Y and Takasu Y 2006 Charge storage mechanism of nanostructured anhydrous and hydrous ruthenium-based oxides *Electrochim. Acta* **52** 1742–8

[22] Hones P, Gerfin T and Grätzel M 1995 Spectroscopic ellipsometry of RuO_2 films prepared by metalorganic chemical vapor deposition *Appl. Phys. Lett.* **67** 3078–80